BABAR-PUB-02/007
SLAC-PUB-9262
hep-ex/0000000

Rare B Decays into States Containing a J/ψ Meson and a Meson with $s\bar{s}$ Quark Content

B. Aubert,[1] D. Boutigny,[1] J.-M. Gaillard,[1] A. Hicheur,[1] Y. Karyotakis,[1] J. P. Lees,[1] P. Robbe,[1] V. Tisserand,[1] A. Zghiche,[1] A. Palano,[2] A. Pompili,[2] J. C. Chen,[3] N. D. Qi,[3] G. Rong,[3] P. Wang,[3] Y. S. Zhu,[3] G. Eigen,[4] I. Ofte,[4] B. Stugu,[4] G. S. Abrams,[5] A. W. Borgland,[5] A. B. Breon,[5] D. N. Brown,[5] J. Button-Shafer,[5] R. N. Cahn,[5] E. Charles,[5] M. S. Gill,[5] A. V. Gritsan,[5] Y. Groysman,[5] R. G. Jacobsen,[5] R. W. Kadel,[5] J. Kadyk,[5] L. T. Kerth,[5] Yu. G. Kolomensky,[5] J. F. Kral,[5] C. LeClerc,[5] M. E. Levi,[5] G. Lynch,[5] L. M. Mir,[5] P. J. Oddone,[5] T. J. Orimoto,[5] M. Pripstein,[5] N. A. Roe,[5] A. Romosan,[5] M. T. Ronan,[5] V. G. Shelkov,[5] A. V. Telnov,[5] W. A. Wenzel,[5] T. J. Harrison,[6] C. M. Hawkes,[6] D. J. Knowles,[6] S. W. O'Neale,[6] R. C. Penny,[6] A. T. Watson,[6] N. K. Watson,[6] T. Deppermann,[7] K. Goetzen,[7] H. Koch,[7] B. Lewandowski,[7] K. Peters,[7] H. Schmuecker,[7] M. Steinke,[7] N. R. Barlow,[8] W. Bhimji,[8] J. T. Boyd,[8] N. Chevalier,[8] P. J. Clark,[8] W. N. Cottingham,[8] C. Mackay,[8] F. F. Wilson,[8] K. Abe,[9] C. Hearty,[9] T. S. Mattison,[9] J. A. McKenna,[9] D. Thiessen,[9] S. Jolly,[10] A. K. McKemey,[10] V. E. Blinov,[11] A. D. Bukin,[11] A. R. Buzykaev,[11] V. B. Golubev,[11] V. N. Ivanchenko,[11] A. A. Korol,[11] E. A. Kravchenko,[11] A. P. Onuchin,[11] S. I. Serednyakov,[11] Yu. I. Skovpen,[11] A. N. Yushkov,[11] D. Best,[12] M. Chao,[12] D. Kirkby,[12] A. J. Lankford,[12] M. Mandelkern,[12] S. McMahon,[12] D. P. Stoker,[12] K. Arisaka,[13] C. Buchanan,[13] S. Chun,[13] D. B. MacFarlane,[14] S. Prell,[14] Sh. Rahatlou,[14] G. Raven,[14] V. Sharma,[14] J. W. Berryhill,[15] C. Campagnari,[15] B. Dahmes,[15] P. A. Hart,[15] N. Kuznetsova,[15] S. L. Levy,[15] O. Long,[15] A. Lu,[15] M. A. Mazur,[15] J. D. Richman,[15] W. Verkerke,[15] J. Beringer,[16] A. M. Eisner,[16] M. Grothe,[16] C. A. Heusch,[16] W. S. Lockman,[16] T. Pulliam,[16] T. Schalk,[16] R. E. Schmitz,[16] B. A. Schumm,[16] A. Seiden,[16] M. Turri,[16] W. Walkowiak,[16] D. C. Williams,[16] M. G. Wilson,[16] E. Chen,[17] G. P. Dubois-Felsmann,[17] A. Dvoretskii,[17] D. G. Hitlin,[17] F. C. Porter,[17] A. Ryd,[17] A. Samuel,[17] S. Yang,[17] S. Jayatilleke,[18] G. Mancinelli,[18] B. T. Meadows,[18] M. D. Sokoloff,[18] T. Barillari,[19] P. Bloom,[19] W. T. Ford,[19] U. Nauenberg,[19] A. Olivas,[19] P. Rankin,[19] J. Roy,[19] J. G. Smith,[19] W. C. van Hoek,[19] L. Zhang,[19] J. Blouw,[20] J. L. Harton,[20] M. Krishnamurthy,[20] A. Soffer,[20] W. H. Toki,[20] R. J. Wilson,[20] J. Zhang,[20] D. Altenburg,[21] T. Brandt,[21] J. Brose,[21] T. Colberg,[21] M. Dickopp,[21] R. S. Dubitzky,[21] A. Hauke,[21] E. Maly,[21] R. Müller-Pfefferkorn,[21] S. Otto,[21] K. R. Schubert,[21] R. Schwierz,[21] B. Spaan,[21] L. Wilden,[21] D. Bernard,[22] G. R. Bonneaud,[22] F. Brochard,[22] J. Cohen-Tanugi,[22] S. Ferrag,[22] S. T'Jampens,[22] Ch. Thiebaux,[22] G. Vasileiadis,[22] M. Verderi,[22] A. Anjomshoaa,[23] R. Bernet,[23] A. Khan,[23] D. Lavin,[23] F. Muheim,[23] S. Playfer,[23] J. E. Swain,[23] J. Tinslay,[23] M. Falbo,[24] C. Borean,[25] C. Bozzi,[25] L. Piemontese,[25] A. Sarti,[25] E. Treadwell,[26] F. Anulli,[27,*] R. Baldini-Ferroli,[27] A. Calcaterra,[27] R. de Sangro,[27] D. Falciai,[27] G. Finocchiaro,[27] P. Patteri,[27] I. M. Peruzzi,[27,*] M. Piccolo,[27] A. Zallo,[27] S. Bagnasco,[28] A. Buzzo,[28] R. Contri,[28] G. Crosetti,[28] M. Lo Vetere,[28] M. Macri,[28] M. R. Monge,[28] S. Passaggio,[28] F. C. Pastore,[28] C. Patrignani,[28] E. Robutti,[28] A. Santroni,[28] S. Tosi,[28] M. Morii,[29] R. Bartoldus,[30] G. J. Grenier,[30] U. Mallik,[30] J. Cochran,[31] H. B. Crawley,[31] J. Lamsa,[31] W. T. Meyer,[31] E. I. Rosenberg,[31] J. Yi,[31] M. Davier,[32] G. Grosdidier,[32] A. Höcker,[32] H. M. Lacker,[32] S. Laplace,[32] F. Le Diberder,[32] V. Lepeltier,[32] A. M. Lutz,[32] T. C. Petersen,[32] S. Plaszczynski,[32] M. H. Schune,[32] L. Tantot,[32] S. Trincaz-Duvoid,[32] G. Wormser,[32] R. M. Bionta,[33] V. Brigljević,[33] D. J. Lange,[33] M. Mugge,[33] K. van Bibber,[33] D. M. Wright,[33] A. J. Bevan,[34] J. R. Fry,[34] E. Gabathuler,[34] R. Gamet,[34] M. George,[34] M. Kay,[34] D. J. Payne,[34] R. J. Sloane,[34] C. Touramanis,[34] M. L. Aspinwall,[35] D. A. Bowerman,[35] P. D. Dauncey,[35] U. Egede,[35] I. Eschrich,[35] G. W. Morton,[35] J. A. Nash,[35] P. Sanders,[35] D. Smith,[35] G. P. Taylor,[35] J. J. Back,[36] G. Bellodi,[36] P. Dixon,[36] P. F. Harrison,[36] R. J. L. Potter,[36] H. W. Shorthouse,[36] P. Strother,[36] P. B. Vidal,[36] G. Cowan,[37] H. U. Flaecher,[37] S. George,[37] M. G. Green,[37] A. Kurup,[37] C. E. Marker,[37] T. R. McMahon,[37] S. Ricciardi,[37] F. Salvatore,[37] G. Vaitsas,[37] M. A. Winter,[37] D. Brown,[38] C. L. Davis,[38] J. Allison,[39] R. J. Barlow,[39] A. C. Forti,[39] F. Jackson,[39] G. D. Lafferty,[39] N. Savvas,[39] J. H. Weatherall,[39] J. C. Williams,[39] A. Farbin,[40] A. Jawahery,[40] V. Lillard,[40] D. A. Roberts,[40] J. R. Schieck,[40] G. Blaylock,[41] C. Dallapiccola,[41] K. T. Flood,[41] S. S. Hertzbach,[41] R. Kofler,[41] V. B. Koptchev,[41] T. B. Moore,[41] H. Staengle,[41] S. Willocq,[41] B. Brau,[42] R. Cowan,[42] G. Sciolla,[42] F. Taylor,[42] R. K. Yamamoto,[42] M. Milek,[43]

P. M. Patel,[43] F. Palombo,[44] J. M. Bauer,[45] L. Cremaldi,[45] V. Eschenburg,[45] R. Kroeger,[45] J. Reidy,[45] D. A. Sanders,[45] D. J. Summers,[45] C. Hast,[46] P. Taras,[46] H. Nicholson,[47] C. Cartaro,[48] N. Cavallo,[48] G. De Nardo,[48] F. Fabozzi,[48] C. Gatto,[48] L. Lista,[48] P. Paolucci,[48] D. Piccolo,[48] C. Sciacca,[48] J. M. LoSecco,[49] J. R. G. Alsmiller,[50] T. A. Gabriel,[50] J. Brau,[51] R. Frey,[51] M. Iwasaki,[51] C. T. Potter,[51] N. B. Sinev,[51] D. Strom,[51] E. Torrence,[51] F. Colecchia,[52] A. Dorigo,[52] F. Galeazzi,[52] M. Margoni,[52] M. Morandin,[52] M. Posocco,[52] M. Rotondo,[52] F. Simonetto,[52] R. Stroili,[52] C. Voci,[52] M. Benayoun,[53] H. Briand,[53] J. Chauveau,[53] P. David,[53] Ch. de la Vaissière,[53] L. Del Buono,[53] O. Hamon,[53] Ph. Leruste,[53] J. Ocariz,[53] M. Pivk,[53] L. Roos,[53] J. Stark,[53] P. F. Manfredi,[54] V. Re,[54] V. Speziali,[54] L. Gladney,[55] Q. H. Guo,[55] J. Panetta,[55] C. Angelini,[56] G. Batignani,[56] S. Bettarini,[56] M. Bondioli,[56] F. Bucci,[56] G. Calderini,[56] E. Campagna,[56] M. Carpinelli,[56] F. Forti,[56] M. A. Giorgi,[56] A. Lusiani,[56] G. Marchiori,[56] F. Martinez-Vidal,[56] M. Morganti,[56] N. Neri,[56] E. Paoloni,[56] M. Rama,[56] G. Rizzo,[56] F. Sandrelli,[56] G. Triggiani,[56] J. Walsh,[56] M. Haire,[57] D. Judd,[57] K. Paick,[57] L. Turnbull,[57] D. E. Wagoner,[57] J. Albert,[58] P. Elmer,[58] C. Lu,[58] V. Miftakov,[58] J. Olsen,[58] S. F. Schaffner,[58] A. J. S. Smith,[58] A. Tumanov,[58] E. W. Varnes,[58] F. Bellini,[59] G. Cavoto,[58,59] D. del Re,[14,59] R. Faccini,[14,59] F. Ferrarotto,[59] F. Ferroni,[59] E. Leonardi,[59] M. A. Mazzoni,[59] S. Morganti,[59] G. Piredda,[59] F. Safai Tehrani,[59] M. Serra,[59] C. Voena,[59] S. Christ,[60] G. Wagner,[60] R. Waldi,[60] T. Adye,[61] N. De Groot,[61] B. Franek,[61] N. I. Geddes,[61] G. P. Gopal,[61] S. M. Xella,[61] R. Aleksan,[62] S. Emery,[62] A. Gaidot,[62] P.-F. Giraud,[62] G. Hamel de Monchenault,[62] W. Kozanecki,[62] M. Langer,[62] G. W. London,[62] B. Mayer,[62] G. Schott,[62] B. Serfass,[62] G. Vasseur,[62] Ch. Yeche,[62] M. Zito,[62] M. V. Purohit,[63] A. W. Weidemann,[63] F. X. Yumiceva,[63] I. Adam,[64] D. Aston,[64] N. Berger,[64] A. M. Boyarski,[64] M. R. Convery,[64] D. P. Coupal,[64] D. Dong,[64] J. Dorfan,[64] W. Dunwoodie,[64] R. C. Field,[64] T. Glanzman,[64] S. J. Gowdy,[64] E. Grauges,[64] T. Haas,[64] T. Hadig,[64] V. Halyo,[64] T. Himel,[64] T. Hryn'ova,[64] M. E. Huffer,[64] W. R. Innes,[64] C. P. Jessop,[64] M. H. Kelsey,[64] P. Kim,[64] M. L. Kocian,[64] U. Langenegger,[64] D. W. G. S. Leith,[64] S. Luitz,[64] V. Luth,[64] H. L. Lynch,[64] H. Marsiske,[64] S. Menke,[64] R. Messner,[64] D. R. Muller,[64] C. P. O'Grady,[64] V. E. Ozcan,[64] A. Perazzo,[64] M. Perl,[64] S. Petrak,[64] B. N. Ratcliff,[64] S. H. Robertson,[64] A. Roodman,[64] A. A. Salnikov,[64] T. Schietinger,[64] R. H. Schindler,[64] J. Schwiening,[64] G. Simi,[64] A. Snyder,[64] A. Soha,[64] S. M. Spanier,[64] J. Stelzer,[64] D. Su,[64] M. K. Sullivan,[64] H. A. Tanaka,[64] J. Va'vra,[64] S. R. Wagner,[64] M. Weaver,[64] A. J. R. Weinstein,[64] W. J. Wisniewski,[64] D. H. Wright,[64] C. C. Young,[64] P. R. Burchat,[65] C. H. Cheng,[65] T. I. Meyer,[65] C. Roat,[65] R. Henderson,[66] W. Bugg,[67] H. Cohn,[67] J. M. Izen,[68] I. Kitayama,[68] X. C. Lou,[68] F. Bianchi,[69] M. Bona,[69] D. Gamba,[69] L. Bosisio,[70] G. Della Ricca,[70] S. Dittongo,[70] L. Lanceri,[70] P. Poropat,[70] L. Vitale,[70] G. Vuagnin,[70] R. S. Panvini,[71] S. W. Banerjee,[72] C. M. Brown,[72] D. Fortin,[72] P. D. Jackson,[72] R. Kowalewski,[72] J. M. Roney,[72] H. R. Band,[73] S. Dasu,[73] M. Datta,[73] A. M. Eichenbaum,[73] H. Hu,[73] J. R. Johnson,[73] R. Liu,[73] F. Di Lodovico,[73] A. Mohapatra,[73] Y. Pan,[73] R. Prepost,[73] I. J. Scott,[73] S. J. Sekula,[73] J. H. von Wimmersperg-Toeller,[73] J. Wu,[73] S. L. Wu,[73] Z. Yu,[73] and H. Neal[74]

(The *BABAR* Collaboration)

[1]*Laboratoire de Physique des Particules, F-74941 Annecy-le-Vieux, France*
[2]*Università di Bari, Dipartimento di Fisica and INFN, I-70126 Bari, Italy*
[3]*Institute of High Energy Physics, Beijing 100039, China*
[4]*University of Bergen, Inst. of Physics, N-5007 Bergen, Norway*
[5]*Lawrence Berkeley National Laboratory and University of California, Berkeley, CA 94720, USA*
[6]*University of Birmingham, Birmingham, B15 2TT, United Kingdom*
[7]*Ruhr Universität Bochum, Institut für Experimentalphysik 1, D-44780 Bochum, Germany*
[8]*University of Bristol, Bristol BS8 1TL, United Kingdom*
[9]*University of British Columbia, Vancouver, BC, Canada V6T 1Z1*
[10]*Brunel University, Uxbridge, Middlesex UB8 3PH, United Kingdom*
[11]*Budker Institute of Nuclear Physics, Novosibirsk 630090, Russia*
[12]*University of California at Irvine, Irvine, CA 92697, USA*
[13]*University of California at Los Angeles, Los Angeles, CA 90024, USA*
[14]*University of California at San Diego, La Jolla, CA 92093, USA*
[15]*University of California at Santa Barbara, Santa Barbara, CA 93106, USA*
[16]*University of California at Santa Cruz, Institute for Particle Physics, Santa Cruz, CA 95064, USA*
[17]*California Institute of Technology, Pasadena, CA 91125, USA*
[18]*University of Cincinnati, Cincinnati, OH 45221, USA*
[19]*University of Colorado, Boulder, CO 80309, USA*
[20]*Colorado State University, Fort Collins, CO 80523, USA*
[21]*Technische Universität Dresden, Institut für Kern- und Teilchenphysik, D-01062 Dresden, Germany*
[22]*Ecole Polytechnique, LLR, F-91128 Palaiseau, France*

[23]University of Edinburgh, Edinburgh EH9 3JZ, United Kingdom
[24]Elon University, Elon University, NC 27244-2010, USA
[25]Università di Ferrara, Dipartimento di Fisica and INFN, I-44100 Ferrara, Italy
[26]Florida A&M University, Tallahassee, FL 32307, USA
[27]Laboratori Nazionali di Frascati dell'INFN, I-00044 Frascati, Italy
[28]Università di Genova, Dipartimento di Fisica and INFN, I-16146 Genova, Italy
[29]Harvard University, Cambridge, MA 02138, USA
[30]University of Iowa, Iowa City, IA 52242, USA
[31]Iowa State University, Ames, IA 50011-3160, USA
[32]Laboratoire de l'Accélérateur Linéaire, F-91898 Orsay, France
[33]Lawrence Livermore National Laboratory, Livermore, CA 94550, USA
[34]University of Liverpool, Liverpool L69 3BX, United Kingdom
[35]University of London, Imperial College, London, SW7 2BW, United Kingdom
[36]Queen Mary, University of London, E1 4NS, United Kingdom
[37]University of London, Royal Holloway and Bedford New College, Egham, Surrey TW20 0EX, United Kingdom
[38]University of Louisville, Louisville, KY 40292, USA
[39]University of Manchester, Manchester M13 9PL, United Kingdom
[40]University of Maryland, College Park, MD 20742, USA
[41]University of Massachusetts, Amherst, MA 01003, USA
[42]Massachusetts Institute of Technology, Laboratory for Nuclear Science, Cambridge, MA 02139, USA
[43]McGill University, Montréal, QC, Canada H3A 2T8
[44]Università di Milano, Dipartimento di Fisica and INFN, I-20133 Milano, Italy
[45]University of Mississippi, University, MS 38677, USA
[46]Université de Montréal, Laboratoire René J. A. Lévesque, Montréal, QC, Canada H3C 3J7
[47]Mount Holyoke College, South Hadley, MA 01075, USA
[48]Università di Napoli Federico II, Dipartimento di Scienze Fisiche and INFN, I-80126, Napoli, Italy
[49]University of Notre Dame, Notre Dame, IN 46556, USA
[50]Oak Ridge National Laboratory, Oak Ridge, TN 37831, USA
[51]University of Oregon, Eugene, OR 97403, USA
[52]Università di Padova, Dipartimento di Fisica and INFN, I-35131 Padova, Italy
[53]Universités Paris VI et VII, Lab de Physique Nucléaire H. E., F-75252 Paris, France
[54]Università di Pavia, Dipartimento di Elettronica and INFN, I-27100 Pavia, Italy
[55]University of Pennsylvania, Philadelphia, PA 19104, USA
[56]Università di Pisa, Scuola Normale Superiore and INFN, I-56010 Pisa, Italy
[57]Prairie View A&M University, Prairie View, TX 77446, USA
[58]Princeton University, Princeton, NJ 08544, USA
[59]Università di Roma La Sapienza, Dipartimento di Fisica and INFN, I-00185 Roma, Italy
[60]Universität Rostock, D-18051 Rostock, Germany
[61]Rutherford Appleton Laboratory, Chilton, Didcot, Oxon, OX11 0QX, United Kingdom
[62]DAPNIA, Commissariat à l'Energie Atomique/Saclay, F-91191 Gif-sur-Yvette, France
[63]University of South Carolina, Columbia, SC 29208, USA
[64]Stanford Linear Accelerator Center, Stanford, CA 94309, USA
[65]Stanford University, Stanford, CA 94305-4060, USA
[66]TRIUMF, Vancouver, BC, Canada V6T 2A3
[67]University of Tennessee, Knoxville, TN 37996, USA
[68]University of Texas at Dallas, Richardson, TX 75083, USA
[69]Università di Torino, Dipartimento di Fisica Sperimentale and INFN, I-10125 Torino, Italy
[70]Università di Trieste, Dipartimento di Fisica and INFN, I-34127 Trieste, Italy
[71]Vanderbilt University, Nashville, TN 37235, USA
[72]University of Victoria, Victoria, BC, Canada V8W 3P6
[73]University of Wisconsin, Madison, WI 53706, USA
[74]Yale University, New Haven, CT 06511, USA

(Dated: August 7, 2012)

We report a study of the B meson decays, $B^+ \to J/\psi\phi K^+$, $B^0 \to J/\psi\phi K^0_S$, $B^0 \to J/\psi\phi$, $B^0 \to J/\psi\eta$ and $B^0 \to J/\psi\eta'$ using 56 million $B\overline{B}$ events collected at the $\Upsilon(4S)$ resonance with the *BABAR* detector at the PEP-II e^+e^- asymmetric-energy storage ring. We measure the branching fractions $\mathcal{B}(B^+ \to J/\psi\phi K^+) = (4.4 \pm 1.4(stat) \pm 0.5(syst)) \times 10^{-5}$ and $\mathcal{B}(B^0 \to J/\psi\phi K^0_S) = (5.1 \pm 1.9(stat) \pm 0.5(syst)) \times 10^{-5}$, and set upper limits at 90% confidence level for the branching fractions $\mathcal{B}(B^0 \to J/\psi\phi) < 9.2 \times 10^{-6}$, $\mathcal{B}(B^0 \to J/\psi\eta) < 2.7 \times 10^{-5}$, and $\mathcal{B}(B^0 \to J/\psi\eta') < 6.3 \times 10^{-5}$.

PACS numbers: 13.25.Hw, 12.15.Hh, 11.30.Er

Recent observations of the B meson decays $B \to J/\psi\pi$ [1] and $J/\psi\rho$ [2] are evidence for the Cabibbo-

suppressed transition $b \to c\overline{c}d$ via the color-suppressed diagram shown in Fig. 1 (a). Here we present a search for color-suppressed modes with hidden strangeness, $s\overline{s}$, in the final state: $B \to J/\psi\eta, J/\psi\eta', J/\psi\phi$ and $J/\psi\phi K$. The decays $B^0 \to J/\psi\eta$ and $B^0 \to J/\psi\eta'$ occur via the same diagram, Fig. 1 (a), and should have a rate comparable to $B \to J/\psi\pi$. If large enough samples can be isolated, these CP eigenstates could be used to test CP violation [3]. Models based on the heavy quark factorization approximation by A. Deandrea *et al.* [4] are used to predict that the branching fraction for $B^0 \to J/\psi\eta$ is a factor of 4 smaller than that for $B^0 \to J/\psi\pi^0$. Assuming that the decay $B^0 \to J/\psi\phi$ is a color-suppressed mode with rescattering as shown in Fig. 1 (b), then the absence of a signal would indicate that the rescattering effects are negligible. The decay $B \to J/\psi\phi K$ is a Cabibbo-allowed and color-suppressed decay via the transition $b\overline{q} \to c\overline{c}s\overline{s}s\overline{q}$, where the $s\overline{s}$ quark pairs are produced from sea quarks or are connected via gluons as shown in Figs. 1 (c) and (d), respectively. This particular three-body decay would be of interest in the search for hybrid charmonium states that decay to the final state $J/\psi\phi$ [5]. In this paper we report on branching fractions or upper limits for $J/\psi\eta$, $J/\psi\eta'$, $J/\psi\phi$, $J/\psi\phi K^+$, and $J/\psi\phi K^0_S$.

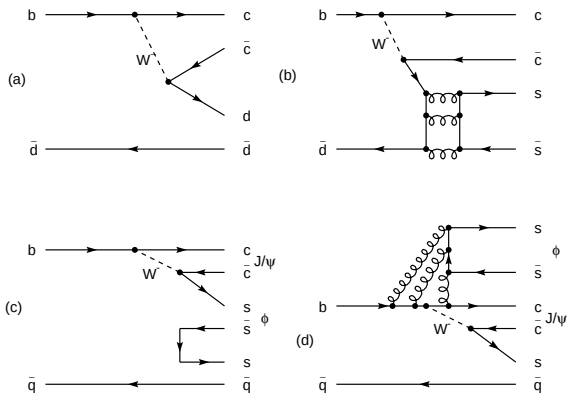

FIG. 1: Quark diagrams: (a) tree diagram for $B \to J/\psi\pi$ and $J/\psi\rho$, (b) rescattering for $B \to J/\psi\phi$, (c) strange sea quarks and (d) gluon coupling for $B \to J/\psi\phi K$.

The data used in this analysis were collected at the PEP-II asymmetric-energy e^+e^- storage ring with the *BABAR* detector, fully described elsewhere [6]. The *BABAR* detector contains a five-layer silicon vertex tracker (SVT) and a forty-layer drift chamber (DCH) in a 1.5-T solenoidal magnetic field. These devices detect charged particles and measure their momentum and energy loss. Photons and neutral hadrons are detected in a CsI(Tl) crystal electromagnetic calorimeter (EMC). The EMC detects photons with energies as low as 20 MeV and identifies electrons by their energy deposition. An internally reflecting ring-imaging Cherenkov detector (DIRC) of quartz bars is dedicated to charged particle identification (PID). Penetrating muons and neutral hadrons are identified by the steel flux return (IFR), which is instrumented with 18-19 layers of resistive plate chambers.

The data correspond to a total integrated luminosity of 50.9 fb^{-1} taken on the $\Upsilon(4S)$ resonance and 6.3 fb^{-1} taken off-resonance at an energy 0.04 GeV below the $\Upsilon(4S)$ mass and below the threshold for $B\overline{B}$ production. In this sample, there are 55.5 ± 0.6 million $B\overline{B}$ events ($N_{B\overline{B}}$).

In this analysis, all charged track candidates are required to have at least 12 DCH hits and transverse momentum greater than 100 MeV/c. The track candidates not associated with a K^0_S decay must also originate near the nominal beam spot. The muon, electron, and kaon candidates must have a polar angle in radians of $0.3 < \theta_\mu < 2.7$, $0.410 < \theta_e < 2.409$, and $0.45 < \theta_K < 2.50$, respectively. In addition, all charged kaon candidates are required to have a laboratory momentum greater than 250 MeV/c. These requirements ensure the selection of tracks in the regions where the acceptance is well understood by the PID systems.

Photon candidates are identified from energy deposited in contiguous EMC crystals, summed together to form a cluster with total energy greater than 30 MeV and a shower shape consistent with that expected for electromagnetic showers.

Electron candidates are required to have a good match between the expected and measured energy loss ($\mathrm{d}E/\mathrm{d}x$) in the DCH, and between the expected and measured Cherenkov angle in the DIRC. The measurements of the ratio of EMC shower energy to DCH momentum, and the number of EMC crystals associated with the track candidate must be appropriate for an electron.

Muons are selected based on the energy deposited in the EMC, the number and distribution of hits in the IFR, the match between the IFR hits and the extrapolation of the DCH track into the IFR, and the depth of penetration of the track into the IFR.

Charged kaon and pion candidates are selected based on energy loss information from the SVT and DCH and the Cherenkov angle measured by the DIRC.

The intermediate states in the indicated decay modes used in this analysis, $J/\psi\,(ee, \mu\mu)$, $\phi\,(K^+K^-)$, $\eta(\gamma\gamma, \pi^+\pi^-\pi^0)$, $\eta'\,(\eta\,(\gamma\gamma)\,\pi^+\pi^-)$, $\pi^0\,(\gamma\gamma)$, and $K^0_S\,(\pi^+\pi^-)$, are selected with the mass intervals in Table I. Since $B^0 \to J/\psi\eta$ and $B^0 \to J/\psi\eta'$ involve decays of a pseudoscalar meson into a vector and a pseudoscalar meson, the angular distribution is proportional to $\sin^2\theta_\ell$, where θ_ℓ is the helicity angle [11] of the lepton from the J/ψ. Hence an additional requirement of $|\cos\theta_\ell| < 0.8$ is applied to reject continuum and other backgrounds. The η candidates are rejected if either of the associated photons, in combination with any other photon in the event, forms a $\gamma\gamma$ mass within 20 MeV/c^2

of the π^0 mass. For the mode $B^0 \to J/\psi\eta(\gamma\gamma)$, the η candidate is required to have $\left|\cos\theta_\gamma^\eta\right| < 0.8$, where θ_γ^η is the photon helicity angle in the η rest frame. This rejects combinatoric background due to random pairs of photons that typically have a photon helicity angle that peaks at 0 or 180 degrees. For the $\eta' \to \eta\,(\gamma\gamma)\,\pi^+\pi^-$ candidates, we use the same η selection criteria for the η described above, including the π^0 veto.

An additional requirement is applied to separate two-jet continuum events from the more spherical B meson decays. The angle θ_T between the thrust direction of the B meson candidate and the thrust direction of the remaining tracks in the event is calculated. We require $|\cos\theta_T| < 0.8$, since these thrust axes are uncorrelated and the distribution in $\cos\theta_T$ is flat for $B\overline{B}$ events, while the distribution is peaked at $\cos\theta_T = \pm 1$ for continuum events.

TABLE I: Mass regions for selection of intermediate particles.

Mode	Mass Range (GeV/c^2)
$J/\psi \to e^+e^-$	$2.95 < M(e^+e^-) < 3.14$
$J/\psi \to \mu^+\mu^-$	$3.06 < M\left(\mu^+\mu^-\right) < 3.14$
$\phi \to K^+K^-$	$1.004 < M\left(K^+K^-\right) < 1.034$
$K^0_S \to \pi^+\pi^-$	$0.489 < M\left(\pi^+\pi^-\right) < 0.507$
$\eta \to \gamma\gamma$	$0.529 < M\left(\gamma\gamma\right) < 0.565$
$\eta \to \pi^+\pi^-\pi^0$	$0.529 < M\left(\pi^+\pi^-\pi^0\right) < 0.565$
$\eta' \to \eta\pi^+\pi^-$	$0.938 < M\left(\eta\pi^+\pi^-\right) < 0.978$
$\pi^0 \to \gamma\gamma$	$0.120 < M\left(\gamma\gamma\right) < 0.150$

The intermediate candidates are combined to construct the B candidates for the six decay modes under study. The estimation of the signal and the background employs two kinematic variables: the energy difference ΔE between the energy of the B candidate and the beam energy E_b^* in the $\Upsilon(4S)$ rest frame; and the energy-substituted mass $m_{\rm ES} = \sqrt{(E_b^*)^2 - (P_B^*)^2}$, where P_B^* is the reconstructed momentum of the B candidate in the $\Upsilon(4S)$ frame. Typically these two weakly correlated variables form a two-dimensional Gaussian distribution for the B meson signal but not for background. The resolutions in ΔE and $m_{\rm ES}$ are decay mode dependent. A signal region for each mode is defined as a rectangular region in the ΔE versus $m_{\rm ES}$ plane, listed in Table II. The $m_{\rm ES}$ range is given in term of $m_{\rm ES} - m_B$, where m_B is the mass of B meson. The number of data events, n_0, observed in the signal region for each mode is listed in Table II.

The efficiencies for each mode are determined by Monte Carlo simulation. The simulations of $J/\psi\phi K$ and $J/\psi\phi$ decays assumed three- and two-body phase space, respectively, with unpolarized J/ψ and ϕ decays. The $J/\psi\eta$ and $J/\psi\eta'$ simulations used the angular correlations determined by the helicity amplitude.

The backgrounds in the $m_{\rm ES}$ distribution are composed of two components: a combinatoric background, whose shape is described by an ARGUS function [7], and a peaking background that peaks in the signal region and is described by a Gaussian function. The sources of combinatoric background are the continuum events and two categories of $B\overline{B}$ events: decays with a leptonic J/ψ decay, and those without. Monte Carlo simulation studies show that the source of the peaking background is $B\overline{B}$ events that contain a leptonic J/ψ decay.

The shape of the ARGUS function is determined mode by mode by fitting to the $m_{\rm ES}$ distribution of candidates in an enhanced fake J/ψ sample, which is obtained by reversing the normal lepton identification requirements.

The normalization of the combinatoric background for each mode is obtained from a fit to the $m_{\rm ES}$ distributions in the ΔE signal region of the on-peak data. The integral of the ARGUS function in the signal region is n_C, the number of combinatoric background events.

The peaking background is determined from a fit to the $m_{\rm ES}$ distribution of Monte Carlo $B\overline{B}$ events with leptonic J/ψ decays using the sum of a Gaussian and an ARGUS function. The number of peaking background events n_P is the integral of the Gaussian function in the signal region.

The total number of background events (n_b) and the uncertainty on this number (σ_b) are calculated from the fit value of n_C and n_P and their errors. The values of n_b and σ_b are listed in Table II for all modes. The combinatoric background is by far the dominant background in all modes except the $B^0 \to J/\psi\eta(\pi^+\pi^-\pi^0)$ mode, where the peaking component is $\sim 20\%$ of the total background.

In Table III, we list the contribution to the systematic error from the uncertainty on each of the following quantities: $N_{B\overline{B}}$; secondary branching fractions [8]; Monte Carlo statistics; PID, tracking, and photon detection efficiencies, which are based on the study of control samples; and background parameterization, which is estimated using ΔE sideband information.

Additional systematic uncertainties due to the decay model dependence are estimated for the modes $J/\psi\phi$, $J/\psi\phi K^+$, and $J/\psi\phi K^0_S$. Monte Carlo simulations are used to determine how much the efficiency depends on assumptions about intermediate resonances and angular distributions. Two samples are generated for each of the three modes with decay distributions determined by the assumed polarization of the vector daughter mesons, rather than by phase space. One sample is generated with 100% transversely polarized J/ψ and ϕ mesons, and the other with 100% longitudinally polarized J/ψ and ϕ mesons. The resulting relative change in efficiency is entered as a fractional systematic error in Table III. An additional check based on Monte Carlo samples with an intermediate state gives negligible effect.

The total systematic error for each mode combines all these separate errors in quadrature and is listed (Total) in Table III.

There is evidence for signals in the $J/\psi\phi K^+$ and

$J/\psi\phi K^0_S$ modes. The results are shown in Figs. 2 and 3. The Poisson probability that the background n_b fluctuates up to the observed number of events, n_0, or higher is 7.7×10^{-6} for $J/\psi\phi K^+$ and 4.2×10^{-5} for $J/\psi\phi K^0_S$. The branching fraction for these modes is determined by a simple subtraction of events in the signal region that yields the number of signal events, $n_s = n_0 - n_b$. The calculation of the branching fraction is based on the efficiency, n_s, $N_{B\overline{B}}$, and the secondary branching fractions for the J/ψ, ϕ, and K^0_S from Ref. [8]. The results are summarized in Table II where the first error is the statistical error and the second is the systematic error, listed in Table III. The derived result for $B^0 \to J/\psi\phi K^0$ is also shown in Table II.

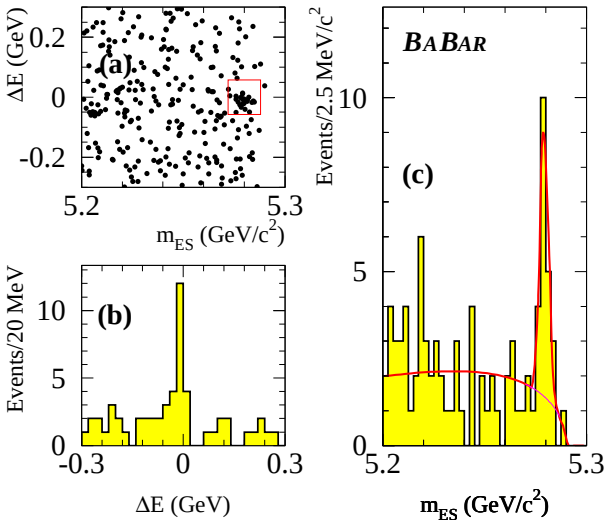

FIG. 2: The ΔE and $m_{\rm ES}$ distributions for $B^+ \to J/\psi\phi K^+$. The ΔE vs. $m_{\rm ES}$ event distribution is shown in (a) with a small rectangle corresponding to the signal region selection defined in Table II. The ΔE projection with a $m_{\rm ES}$ signal region selection is shown in (b). The $m_{\rm ES}$ projection with a ΔE signal region selection is shown in (c). The solid line in (c) is the fit described in the text. The Gaussian component includes both the signal and peaking background.

For modes with no signal or limited statistical evidence ($J/\psi\phi$, $J/\psi\eta$, $J/\psi\eta'$), we determine both a central confidence interval and an upper limit interpretation for the branching fraction. The upper limit method uses n_0, n_b, and σ_b, in the signal region, and the total systematic uncertainty σ_T. Assuming the two uncertainties (σ_b, σ_T) are uncorrelated and Gaussian, the Bayesian upper limit on the number of events ($N_{90\%}$) is obtained by folding the Poisson distribution with two normal distributions for these two uncertainties and integrating it to the 90% confidence level (C.L.). In Table II we list for each mode the efficiency, the number of observed events, the expected number of background events, the 90% C.L. upper limit for observed events, the corresponding branching fraction limit and a central interval for

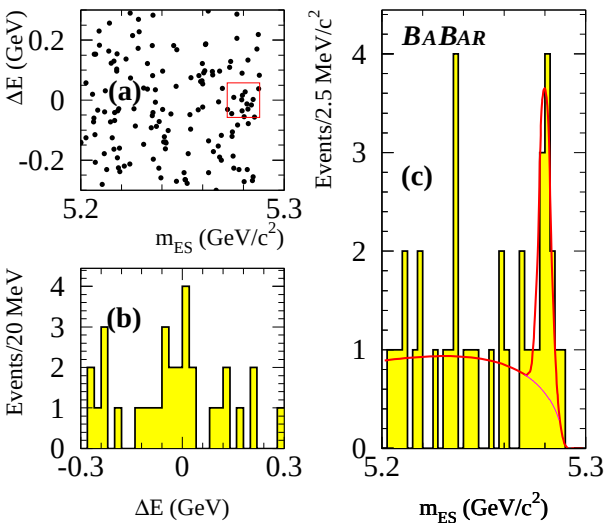

FIG. 3: The ΔE and $m_{\rm ES}$ distributions for $B^0 \to J/\psi\phi K^0_S$. The descriptions of Figs. 3(a), (b) and (c) follow those of Figs. 2(a), (b) and (c), respectively.

the branching fraction. The upper limit obtained from the combination of the two $B^0 \to J/\psi\eta$ modes is shown in Table II. The mean value of the branching fraction is calculated for $B^0 \to J/\psi\phi$ and $B^0 \to J/\psi\eta'$. We also combine the observed numbers of events for the two $B^0 \to J/\psi\eta$ modes to calculate a branching fraction of $(1.6\pm0.6(stat.)\pm0.1(syst.))\times10^{-5}$. The Poisson probability that the background fluctuates up to the observed number of events or higher is 2.5×10^{-5} for the combined result.

In summary, we determine the branching fraction of $B \to J/\psi\phi K$ in two modes, $\mathcal{B}(B^+ \to J/\psi\phi K^+) = (4.4\pm1.4\pm0.5)\times10^{-5}$ and $\mathcal{B}(B^0 \to J/\psi\phi K^0_S) = (5.1\pm1.9\pm0.5)\times10^{-5}$. The branching fraction of $B \to J/\psi\phi K$ is consistent with a CLEO [10] result, $\left(8.8^{+3.5}_{-3.0}\pm1.3\right)\times10^{-5}$. Upper limits have been determined for the modes $B^0 \to J/\psi\phi$, $J/\psi\eta$, and $J/\psi\eta'$. The upper limit on $B^0 \to J/\psi\eta$ is a significant improvement over the previous best limit of $< 1.2\times10^{-3}$ at 90% C.L., from the L3 Collaboration [9]. The combined branching fraction for $B^0 \to J/\psi\eta$ is comparable to the $B^0 \to J/\psi\pi^0$ branching fraction [1]. The search and resulting upper limits on the branching fractions for $B^0 \to J/\psi\eta'$ and $B^0 \to J/\psi\phi$ are presented.

We are grateful for the excellent luminosity and machine conditions provided by our PEP-II colleagues, and for the substantial dedicated effort from the computing organizations that support *BABAR*. The collaborating institutions wish to thank SLAC for its support and kind hospitality. This work is supported by DOE and NSF (USA), NSERC (Canada), IHEP (China), CEA and CNRS-IN2P3 (France), BMBF and DFG (Germany), INFN (Italy), NFR (Norway), MIST (Russia),

TABLE II: Branching fractions and 90% C.L. upper limits.

Mode	Signal Region ΔE (MeV)	Signal Region $\lvert m_{\rm ES} - m_B\rvert$ (MeV/c^2)	Efficiency	n_0	$n_b \pm \sigma_b$	$N_{90\%}$	90% C.L. Upper Limit (10^{-5})	Branching Fraction (10^{-5})
$J/\psi\phi K^+$	57.0	8.0	10.6%	23	7.8 ± 0.6			$4.4 \pm 1.4 \pm 0.5$
$J/\psi\phi K^0_S$	57.0	8.0	8.6%	13	3.3 ± 0.4			$5.1 \pm 1.9 \pm 0.5$
$J/\psi\phi K^0$								$10.2 \pm 3.8 \pm 1.0$
$J/\psi\phi$	57.0	8.0	12.1%	1	0.3 ± 0.2	3.60	< 0.9	$0.18 \pm 0.26 \pm 0.03$
$J/\psi\eta'$	100.0	10.0	2.5%	0	0.5 ± 0.3	1.81	< 6.3	$-1.7 \pm 1.0 \pm 0.2$
$J/\psi\eta\,(\gamma\gamma)$	100.0	10.0	15.5%	8	1.7 ± 0.4	11.5	< 2.9	
$J/\psi\eta\,(\pi^+\pi^-\pi^0)$	72.0	10.0	8.7%	4	1.5 ± 0.9	6.76	< 5.1	
$J/\psi\eta$ combined							< 2.7	$1.6 \pm 0.6 \pm 0.1$

TABLE III: Systematic error summary on the branching fractions. All are fractional uncertainties in percent.

Mode	$N_{B\overline{B}}$	Secondary Branching Fractions	Monte Carlo Statistics	PID, Tracking, Photon Detection	Background Parameterization	Model	Total
$J/\psi\phi K^+$	1.1	2.2	1.6	8.2	5.9	0.4	10.4
$J/\psi\phi K^0_S$	1.1	2.2	2.1	8.3	1.9	0.9	9.3
$J/\psi\phi$	1.1	2.2	1.6	6.7	12.0	1.0	14.1
$J/\psi\eta'$	1.1	3.8	4.6	9.3	7.1	-	13.3
$J/\psi\eta\,(\gamma\gamma)$	1.1	1.8	1.6	6.0	6.9	-	9.5
$J/\psi\eta\,(\pi^+\pi^-\pi^0)$	1.1	2.4	2.2	7.7	8.0	-	11.6

and PPARC (United Kingdom). Individuals have received support from the A. P. Sloan Foundation, Research Corporation, and Alexander von Humboldt Foundation.

* Also with Università di Perugia, I-06100 Perugia, Italy

[1] *BABAR* Collaboration, B. Aubert *et al.*, Phys. Rev. **D65**, 32001 (2002).
[2] CLEO Collaboration, M. Bishai *et al.*, Phys. Lett. **B369**, 186 (1996); *BABAR* Collaboration, hep-ex/0209013, submitted to Phys. Rev. Lett.
[3] M. Beneke, G. Buchalla, and I. Dunietz, Phys. Lett. **B393**, 132 (1997).
[4] A. Deandrea *et al.*, Phys. Lett. **B318**, 549 (1993).
[5] F. E. Close *et al.*, Phys. Rev. **D57**, 5653 (1998).
[6] *BABAR* Collaboration, B. Aubert *et al.*, Nucl. Instr. and Methods **A479**, 1 (2002).
[7] ARGUS Collaboration, H. Albrecht *et al.*, Z. Phys **C48**, 543 (1990).
[8] Particle Data Group, D.E. Groom *et al.*, Eur. Phys. J. C **15**, 1 (2000).
[9] L3 Collaboration, M. Acciarri *et al.*, Phys. Lett. **B391**, 481 (1997).
[10] CLEO Collaboration, A. Anastassov *et al.*, Phys. Rev. Lett. **84**, 1393 (2000).
[11] In the reaction, $Z \to X + Y, X \to a + b$, the helicity angle of particle a is defined as the angle measured in the particle X rest frame between the direction of particle a and the direction opposite to particle Z.